Goodness-of-fit Criteria for Broadband Synthetic Seismograms, with Application to the 2008 M_w 5.4 Chino Hills, California, Earthquake

Kim B. Olsen[1] and John E. Mayhew[1,2]

Online material: Description of metrics and comparison of our goodness-of-fit (GOF) method to other proposed GOF measures.

INTRODUCTION

Broadband synthetics obtained from scenario simulations of earthquakes with a frequency content between 0 and 10 Hz, referred to hereafter as "BBSs," are playing an increasingly important role in seismic hazard analysis. An example is the Great Southern California ShakeOut, the largest disaster response exercise in U.S. history and an annual event since 2008 (Jones *et al.* 2008). The drill was the first to be based on BBSs, in this case for an **M** 7.8 scenario earthquake on the southern San Andreas fault. Another example of the important role of synthetic ground motions is the increasing awareness of the advantages of using site-specific ground-motion time series, rather than empirical intensity measures or scaled time series from different sources or locations, for more realistic non-linear dynamic analysis of buildings and performance-based earthquake engineering. BBSs appear to be one of the only viable alternatives to the very limited amount of strong-motion time series, particularly in the near-field from large earthquakes.

Effectively meeting demands of this sort for realistic BBSs requires careful validation against recorded data. BBSs are currently achieved by combining deterministic low-frequency (LF) synthetics up to a maximum frequency (*fmax)* of typically 1–2 Hz with high-frequency (HF) stochastic synthetics above this upper cutoff frequency (see, for example, Graves and Pitarka 2004; Liu *et al.* 2006; Mai *et al.* forthcoming). Visual inspection has been used for decades to claim success or failure of the ability of simulations to match observations (or synthetics derived from an alternative numerical method). However, at shorter periods such visual waveform fits are not practical, likely due to chaotic source and path variability. For example, specific intensity measures tend to be more practical and relevant than actual waveform fits at higher frequencies.

Candidates for metrics to measure the misfit for BBSs include commonly used ground-motion intensity measures such as peak ground acceleration (PGA), peak ground velocity (PGV), peak ground displacement (PGD), and spectral acceleration (SA), as well as shaking duration—parameters often used by seismologists and earthquake engineers to assess ground motion simulations and estimate building response. For example, Star *et al.* (forthcoming) compared ShakeOut and Puente Hills BBSs (obtained from kinematic source descriptions) to recent Next Generation Attenuation (NGA) relations in terms of PGA, PGV, and SA at several periods. Similarly, Olsen *et al.* (2008, 2009) compared TeraShake and ShakeOut LFs, respectively, obtained from dynamic rupture propagation, to NGA relations in terms of PGV and SA at a period of 3 s. However, if the BBSs are to be used routinely for seismic risk analysis (*e.g.*, the ShakeOut scenario), non-linear dynamic analysis of buildings, or performance-based earthquake engineering, further empirical validation of ground-motion parameters relevant to engineering procedures is required. An example of such a structural engineering-specific metric is the ratio between inelastic and elastic response spectra (IE ratio). As a pioneering effort to demonstrate the usefulness of this metric, Baker and Jayaram (2008, hereafter referred to as BJ08) showed that the mean and standard deviation of IE ratios for a subset of BBSs in the Los Angeles region for several **M** 7.15 scenario earthquakes on the Puente Hills fault (Graves and Somerville 2006) were generally consistent with those for observations. However, they did find discrepancies, particularly at shorter periods, at soft-soil site locations and when strong directivity effects were present in the simulations, and they recommended further study to reconcile these differences. BJ08 is unique in the sense that it focused on properties that are known to affect the response of structures to earthquake ground motion.

In this study we present a new goodness-of-fit (GOF) method for the validation of BBSs, consisting of a combination

1. San Diego State University
2. Now at: ExxonMobil Exploration Company, Houston, Texas

doi: 10.1785/gssrl.81.5.715

of different systematic tests involving commonly used metrics characterizing the fit such as peak ground motions, Fourier and response spectra, cross-correlation, and duration measures. In addition, for structural engineering-specific applications, the GOF algorithm includes a comparison of the IE ratios for the seismograms. A detailed description of the estimation of the metrics and comments on their relevance for the GOF estimate is provided in the electronic supplement. We test the method for BBSs generated for the 2008 M_w 5.4 Chino Hills, California, earthquake.

Two additional GOF measures (Anderson 2004; Kristekova *et al.* 2006) have been proposed for the purpose of validation and verification of synthetic seismograms. These two methods relate to and differ from our proposed GOF measure in important ways. The GOF measure by Kristekova *et al.* compares the differences in the envelope and phase of a pair of seismograms. Their method is best suited for comparison of LF synthetics due to the increasing difficulty in matching the envelope and phase as the upper cut-off frequency increases. For LF comparisons, the Kristekova GOF measure generates a very detailed result illustrating the magnitude and location of the misfit in both time and frequency domains. On the other hand, our GOF measure is primarily designed for validation of BBSs, with less emphasis on detailed LF comparison. For this reason, it is difficult to compare our GOF measure directly to that proposed by Kristekova *et al.* (2006). The GOF measure proposed by Anderson (2004) is meant to compare broadband time series and is similar to our method in many aspects. We provide a more in-depth discussion and comparison of our GOF method to that of Anderson (2004) in the electronic supplement.

GOF ALGORITHM

The basic input for our GOF algorithm consists of one or more pairs of time series to be compared. First, the algorithm increases the number of time samples to a power of two for filtering purposes and fast Fourier transform calculation, and decreases the time step to match the change in the number of time samples or to ensure an un-aliased time step sampling for frequencies up to 15 Hz. The user then chooses between one or several weighted metrics (see the following section) to be included in the GOF estimate. The GOF measure is calculated using the complementary error function (erfc) of a normalized residual NR:

$$\text{GOF} = 100 * \text{erfc}[\text{NR}], \text{ where NR} = \frac{2|x-y|}{x+y}, \qquad (1)$$

where x and y are two sets of positive scalar metrics (discussed in the following section as well as in the electronic supplement). The result (distributed between 0 and 1) is then multiplied by 100 to generate a GOF value between 0 and 100 (perfect fit).

A classification of the GOF values is useful in quantifying the fit values generated based on visual inspection and the ratio between metrics x and y. This ratio (α, see Figure 1 and electronic supplement) is used to facilitate the comparison of our method with that proposed by Anderson (2004). Anderson proposed a classification of his GOF measure based on statistical analysis of randomly generated synthetic seismograms and differences between the horizontal components of recorded seismograms. Based on our experience from the 2008 Chino Hills validation (see below), and in general agreement with Anderson (2004), we propose the following classification of the GOF values calculated by our method: 80–100 ($\alpha \approx 1.0$–1.2) excellent fit, 65–80 ($\alpha \approx 1.2$–1.4) very good fit, 45–65 ($\alpha \approx$ 1.4–1.7) fair fit, and 35–45 ($\alpha \approx 1.7$–2.0) poor fit. The threshold below which the fits are too bad to be considered depends on the specific application and metrics (and their weights) included. In general, we propose to set this threshold around 35 ($\alpha \approx 2.0$). Note that compared to Anderson's method, our approach generates a relatively high-resolution representation of the small misfits, at the expense of a lower resolution at larger misfits (usually of less interest to the user). This desirable shape of the GOF curve was the primary reason for choosing the relatively more complicated erfc in Equation 1, as compared to that used by Anderson (see Figure 1).

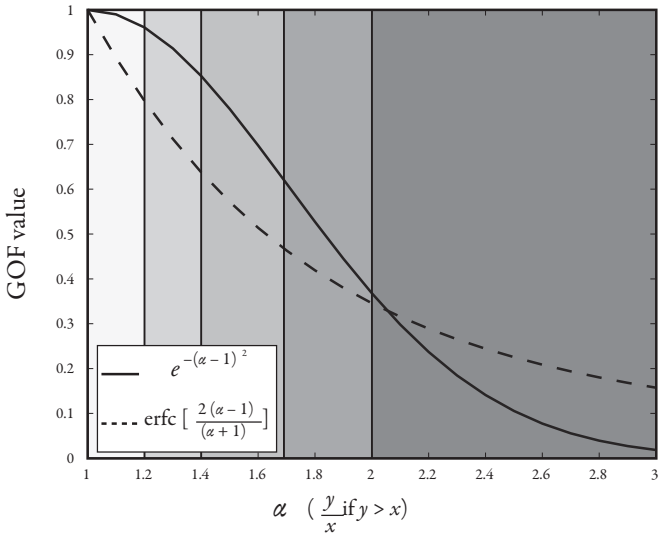

▲ **Figure 1.** A normalized comparison between our proposed GOF measure (solid curve) and that by Anderson (2004) (dashed curve) plotted against the proportionality (α) of the two values being compared. Five areas are highlighted: α = [1–1.2] ("excellent"), [1.2–1.4] ("very good"), [1.4–1.7] ("good"), [1.7–2.0] ("very good"), and [2.0–∞] ("poor").

METRICS

This section identifies the metrics included in our algorithm and discusses how they may be combined at different bandwidths and applications for optimal results. The electronic supplement contains a more in-depth discussion of the metrics.

A ground-motion time series can be described by a variety of different metrics. Some metrics are more meaningful than others for certain applications. Since our algorithm is targeted toward several different purposes, *i.e.*, validation of velocity

models, verification of wave propagation codes, and a test for use of synthetic time histories by structural engineers, a relatively wide selection of metrics is needed. Our algorithm computes GOF values for the following metrics: PGA, PGV, and PGD; the response spectral acceleration averaged for periods between 0.1 and 10 s (RS) as well as the spectral acceleration at 16 individual periods used by recent NGA relations (SA16); the Fourier spectrum (smoothed to reduce variance; FS, Equation S6), energy duration (DUR); cumulative energy (ENER); and cross-correlation (Xcor). These nine metrics are redundant to some degree (discussed in more detail in a later section), and the specific choice of metrics to include in the final GOF estimate is determined for the specific target application as well as from the preference of the user.

The metrics listed above were used in some form by Anderson (2004). In addition, we include a metric that is fundamentally different from those used in previous GOF studies. When exposed to significant seismic motion, inelastic effects begin to dominate the structural response. The IE ratio is the ratio between the maximum inelastic and elastic displacements plotted against the strength reduction factor R. The values of R, the elastic displacement/yield displacement, range from 1 to 10 to provide applicable yield displacements (Tothong and Cornell 2006). We use a post-yield stiffness of 2% of the elastic stiffness (a reasonable value for real buildings; J. Baker, personal communication), although this value can be modified in the GOF method. Our method then calculates a GOF value for each period considered (see Equations S3–S4), based on the relative maximum difference between the recorded and synthetic ratios at each period and within a user-defined bandwidth. A detailed description of our IE GOF metric can be found in the electronic supplement, including a site-specific example calculation (SMS; Figure S1 in the electronic supplement) for the Chino Hills event.

When the evaluated bandwidth is limited to lower frequencies (*e.g.*, <1–2 Hz), the phase of the seismograms becomes more important. This is due to the fact that basic waveform matching is a realistic and often achievable goal in deterministic LF waveform generation. For this reason, the cross-correlation metric (Xcor) is an obvious candidate for LF comparisons. However, we find that time shifts between the same arrivals in the two seismograms under comparison, for example due to errors in the underlying velocity model, can significantly affect the Xcor metric (up to tens of GOF values). The bias from such time shifts can be alleviated by trace alignment. Our experience suggests that, although tedious, manual time shifts to match *S*-wave arrivals are generally considerably more accurate than those obtained automatically by the cross correlation.

As synthetic ground motions are used for engineering purposes, the SA16 and IE calculations can be included to determine the period-dependent level of fit. Large bandwidth comparisons reduce the sensitivity of the IE metric due to generally good fits at long periods (>1 s) and the degradation of fit seen as the period of calculation decreases. Thus, this metric is sensitive to and best suited for period-specific comparisons using narrow bandwidths.

Each of the metrics has an associated weight w_i, which is normalized before it is applied in the average GOF calculation for a specific site:

$$\sum_{i=1}^{N} \varkappa_i \times \mu_i \quad \text{, where } \varkappa_i = \frac{w_i}{\sum_{i=1}^{N} w_i} \tag{2}$$

where μ_i is the GOF value calculated for the ith metric and $\varkappa_i$ is the normalized weight. For our GOF validation for the Chino Hills earthquake we have used a standard equal weighting for the PGA, PGV, PGD, RS, FS, DUR, and ENER metrics to compute the average GOF values. However, the choice of metrics and weights depends on the specific application. A GOF value is estimated independently for each component of the ground motion, and an average value for each metric is calculated from all three components, with the exception of the IE ratio (using only the horizontal components due to engineering conventions; see electronic supplement). We recommend that Xcor be left out of the average BB GOF estimate, unless accurate time shifts have been found, as discussed earlier. Furthermore, we suggest that the IE metric be used primarily for specific structural applications where the GOF calculation is restricted to a narrow bandwidth. The average GOF value is exported along with GOF values for each metric calculated, providing user flexibility in interpreting the results of the algorithm. The electronic supplement provides a comparison of our GOF to that obtained from the method by Anderson (2004), along with details of the GOF computation.

APPLICATION OF OUR GOF MEASURE TO THE 2008 M_w 5.4 CHINO HILLS EARTHQUAKE

We apply our proposed GOF algorithm to compare synthetic and recorded data for the 29 July 2008, M_w 5.4 Chino Hills, California, earthquake, the largest seismic event in the Los Angeles area since the 1994 M_w 6.7 Northridge earthquake. This earthquake was very well recorded on hundreds of seismic stations. The mainshock occurred at a depth of 14.7 km and the epicenter was located in Chino Hills, approximately 28 miles east-southeast of downtown Los Angeles (see Figure 2). The mechanism for this earthquake was a combination of strike-slip and thrust faulting. The 2008 Chino Hills earthquake was felt by many people throughout the Los Angeles basin and the surrounding areas although there was very little damage (Hauksson *et al.* 2008). The largest observed PGA and PGV for the event were 0.44g and 38 cm/s, respectively (CalTrans 2008).

We simulated synthetic waveforms for the 2008 Chino Hills earthquake with a point source (see Table 1), using a fourth-order finite difference method (Olsen 1994) and the Southern California Earthquake Center (SCEC) community velocity model (CVM) version 4.0 (http://epicenter.usc.edu/cmeportal/cmodels.html). The minimum *S*-wave speed in the model was artificially set to 500 m/s for computational purposes, and surface topography was not included. The grid

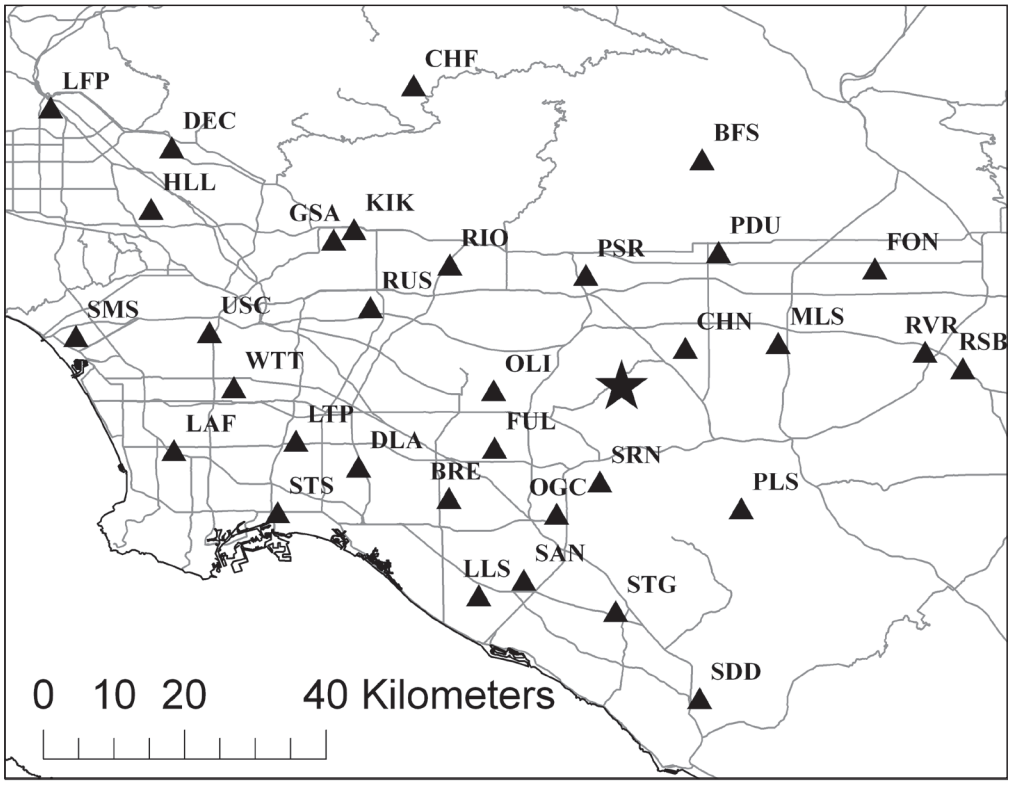

▲ **Figure 2.** Station locations (triangles) where GOF values are estimated for the Chino Hills event. The star depicts the epicenter, lines depict the coastline (black) and major freeways (gray).

TABLE 1
Source Parameters for the 29 July 2008 M_w 5.4 Chino Hills Earthquake

Moment	1.53e17 Nm
Strike	291°
Dip	59°
Rake	142°
Hypocenter	33.953°N, 117.761°W, 14.7 km

spacing was set to 50 m across the model, ensuring an accuracy of at least 6.25 points per minimum shear wavelength for frequencies up to 1.6 Hz. Anelastic attenuation was included using a coarse-grained approach (Day and Bradley 2001), using $Q_s = 50V_s$ (V_s in km/s) and $Q_p = 2Q_s$.

We then generated (0–10Hz) BBSs for the 2008 Chino Hills earthquake using the methods of Mai *et al.* (forthcoming). In this method, broadband synthetic seismograms are computed using a combination of LF deterministic waveforms combined with stochastically generated high-frequency scattering operators ("scatterograms"). The scatterograms are generated using site- and source-specific parameters, and site-specific scattering Green's functions are calculated for an isotropic medium. These scattering Green's functions are then convolved with a source time function (Dreger *et al.* 2007) to generate the HF scatterogram. Finally, the deterministic LFs are combined with the HF scatterograms in the frequency domain within a user-defined bandwidth centered at a source-specific matching frequency (Mai and Beroza 2003). We used a matching frequency of 1.6 Hz ± 0.15 Hz for our BB generation. Time shifts between –1.1 and 0.9 seconds obtained by visual alignment of the primary *S*-wave arrivals in data and synthetics (lowpass-filtered to 1 Hz for easier phase comparison) are applied and included in the GOF calculation. It should be noted that the parameters used for the scattering functions were selected as generic values from the proposed ranges listed by Mena *et al.* (forthcoming); it is possible that an improved fit for the BBSs may be obtained if site-specific parameters (such as kappa and scattering coefficients) were available. The parameters used for BBS generation are summarized in Table 2. The electronic supplement shows 0.1–10.0-Hz BBS velocity waveforms compared to the recorded data for 33 selected stations (see Figure 2 for location).

TABLE 2
Parameters Used by the BB Method by Mai *et al.* (forthcoming) for the Generation of the 2008 Chino Hills BB Synthetics

Matching Frequency	1.6 Hz
Matching Bandwidth	0.3 Hz
Source Time Function	"Dreger"
Source Mechanism	Reverse
Seed number for Scattering Wavelets	4518
Number of Scattering Wavelets	1500
Kappa (site)	0.01 ms
Q (coda waves)	180
Scattering Coefficient (elastic attenuation)	0.01

Average BBS GOF Results

The GOF average of equally weighted PGA, PGV, PGD, RS, FS, DUR, and ENER metrics for the bandwidth 0.1–10 Hz is shown in Figure 3. The best fits (GOF > 60) are found for stations SRN and OGC just south of the epicenter, stations CHF and KIK toward the northwest, and stations HLL and SMS toward the west. Stations with GOF values near or below the proposed acceptable threshold GOF of ~35 include STS (amplitude and duration under-predicted), and stations DEC, PDU, and RVR (amplitude and duration over-predicted).

To further investigate the frequency dependence of the GOF values calculated we analyzed the specific GOF results for PGA and the SAs at two different periods. Figure 4 shows GOF values for PGA and spectral acceleration at periods 0.2 and 2 s. Our comparison shows that in general, the higher-frequency component of the synthetics fit data best at the stations located in the eastern and northern parts of the model area. This is in agreement with the average BBS GOF values (Figure 3), but flags additional stations (*e.g.*, OLI, FUL, and RIO) that may be considered unsuited for specific engineering studies critically dependent on these parameters.

IE Ratio GOF Results

Figure 5(A–C) shows maps of average IE GOF values at A) short periods (0.2–0.5 s), B) moderate periods (0.75–1.5s), and C) long periods (2.0–5.0s), with the IE ratios for synthetics and data at all 33 sites at periods of 0.3 s, 1 s, and 4 s shown in Figure 6. At the shorter periods, about a third of the sites produce GOF values for the IE ratios below the proposed acceptance threshold of ~35 (located primarily north of the epicenter, as well as STG, SMS, and WTT; see Figure 2). On average, the simulated IE ratios are under-predicting the recorded IE ratios at the short periods with a large variance. This is in agreement with the findings by Tothong and Cornell (2006), who showed that the IE ratios for oscillators with a short natural period (<0.6 s) are highly variable. The mean IE values at these periods can reach relatively high values (>3), particularly as R increases. This relationship is due to the fact that the amount of nonlinearity of a structure increases as the natural period decreases, and is related to the inability of short-period structures to dissipate energy effectively (Tothong and Cornell 2006). At moderate periods, the synthetic IE ratios tend to have a very-good to good fit, suggesting that these ground motions could be used in engineering and hazard analysis applications. Finally, the long-period GOF values for the IE ratios are generally very good. Here, the associated IE ratios are relatively small and well determined. The means of the long-period IE ratios tend to be less than one, since longer-period structures (>1.5 s) are relatively unaffected by high levels of nonlinearity. Figure 6 (period of 1.0 s) shows that the mean IE ratios of the data tend to be close to one with a smaller variance as compared to the shorter periods. Moreover, on average, the mean of the synthetics slightly under-predict the mean of the data.

Our finding that the fit between IE ratios for synthetics and data from the Chino Hills event degrades at shorter periods is in agreement with that of BJ08 using Puente Hills scenario simulations and data for other events. However, the Chino Hills study did not show larger discrepancies in IE ratios at soft-soil site locations, as found by BJ08. This result may be due to a bias from the use of a single event in our study (Chino Hills), with a possible directional-dependent soil-amplification pattern.

DISCUSSION AND CONCLUSIONS

We present a new GOF measure for verification and validation of broadband synthetics. Our GOF measure consists of 10 different metrics that can be individually weighted for a specific application. The method is illustrated by comparing broadband (0–10 Hz) synthetics to data for the 2008 M_w 5.4 Chino Hills, California, earthquake, where we find a highly variable fit. Our selected stations just south of the epicenter, toward the northwest and west in the model area, produce the best fits for PGA, SA at 0.2s, and the average BB measure. The worst fits for the shorter periods are generally obtained at our selected stations west of the epicenter. Overall, the BB synthetics for Chino Hills fail to reach our GOF acceptance threshold at about a third of the selected sites. However, it is possible that the use of site-specific parameters (kappa, scattering coefficient) may improve the fit for the shorter periods of the synthetics. Such refinement of the BBSs is left for future work. Moreover, additional stations need to be included in the analysis to draw more solid conclusions on area-specific trends in the GOF patterns.

To illustrate the connection between the temporal and spectral differences for data and synthetics and the associated goodness-of-fit, the fit for the NS component of the broadband waveforms, FS, and RS at stations HLL and PDU are shown in Figure 7. The GOF values for RS, PGV, FS, and the seven-metric average are 67, 75, 82, and 51, respectively, at site HLL (left), and 19, 14, 19, and 11, respectively, at site PDU. GOF comparisons using the IE metric show that for the shorter periods, the simulation matches the recorded data satisfactorily (as defined by our acceptance level of GOF~35) at about two-thirds of the selected sites. At moderate to long periods, the simulated IE ratios are acceptable at all sites, approaching a perfect score at some sites for the longest periods. Thus, the GOF values suggest that the long-period synthetics at all, and short-period BBS at most, of the selected sites have achieved the pre-defined acceptance level. These results are in general agreement with the analysis by BJ08 using synthetics for Puente Hills scenario earthquakes. For future work, we recommend extending our analysis to larger, well-recorded earthquakes, with associated seismic hazards beyond those for the M_w 5.4 Chino Hills event.

Intuitively, the list of the 10 metrics used by our GOF measure is expected to include redundancies. To illustrate this redundancy, Figure 8 shows the correlation matrix of the 10 metrics at the 33 sites used for our analysis of the M_w 5.4 Chino Hills earthquake. RS has the strongest correlation with the other metrics, closely followed by the peak ground motion values (PGA, PGV, and PGD), ENER, and SA16. The least correlated metrics are Xcor, DUR, and IE. It is possible that this correlation pattern depends on sampling parameters such

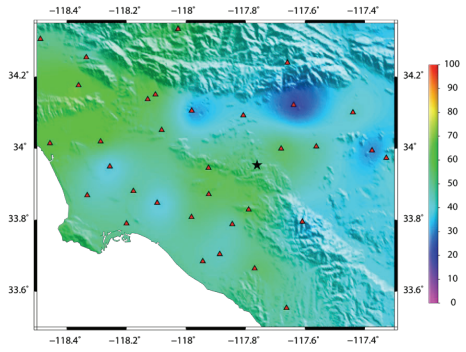

▲ **Figure 3.** Map of average seven-metric (PGA, PGV, PGD, RS, FS, DUR, and ENER) BB (0.1–10 Hz) GOF for the 2008 Chino Hills earthquake. Triangles depict stations used for comparison, and the star depicts the epicenter.

as density of the recording sites and earthquake location. Such dependency should be investigated in future work. A convenient tool to minimize redundancy of the metrics is provided by the weights (Equation 2), and an appropriate set of metrics must be carefully selected for a specific application.

The Chino Hills application could be expanded to illustrate how the GOF algorithm may be used to identify areas of the CVM in need of improvement. In addition, the GOF algorithm could facilitate comparisons of data to synthetics simulated in different CVMs and allow direct assessment of the accuracy of the crustal structure models. Other important applications of the GOF algorithm include comparison of HF generation methods. Such comparison may assist scientists and engineers in determining which of several methods may be better suited for ground-motion prediction. For example, the Community Modeling Environment (CME) group within

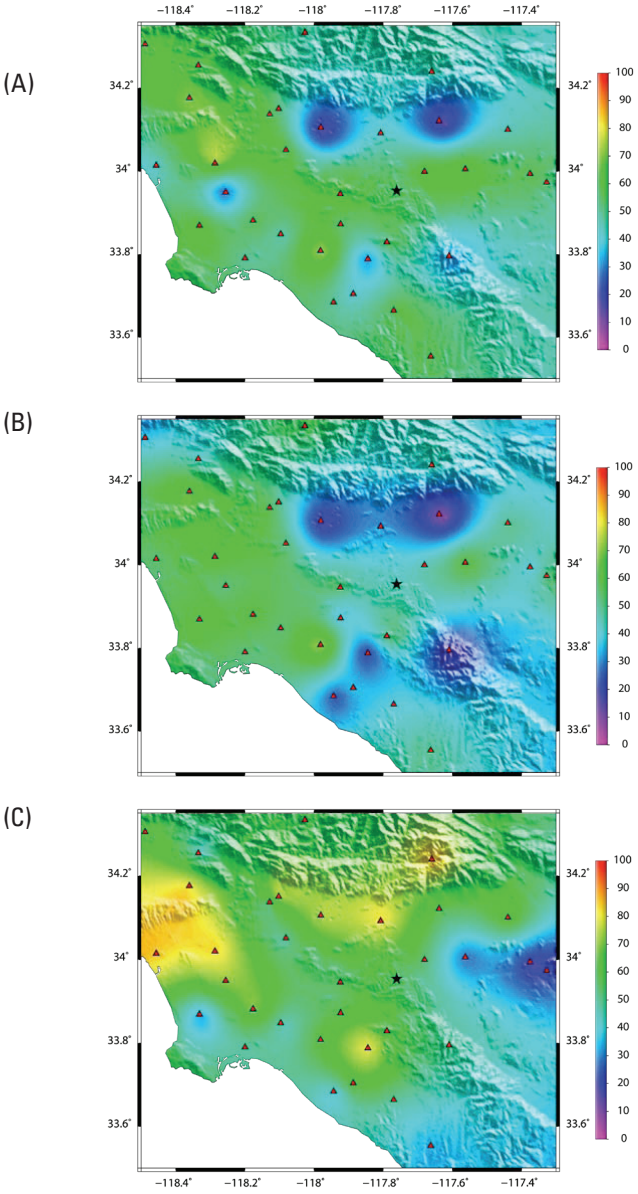

▲ **Figure 4.** Maps of GOF values for A) PGAs and SAs at B) 0.2 s and C) 2.0 s for the 2008 Chino Hills event.

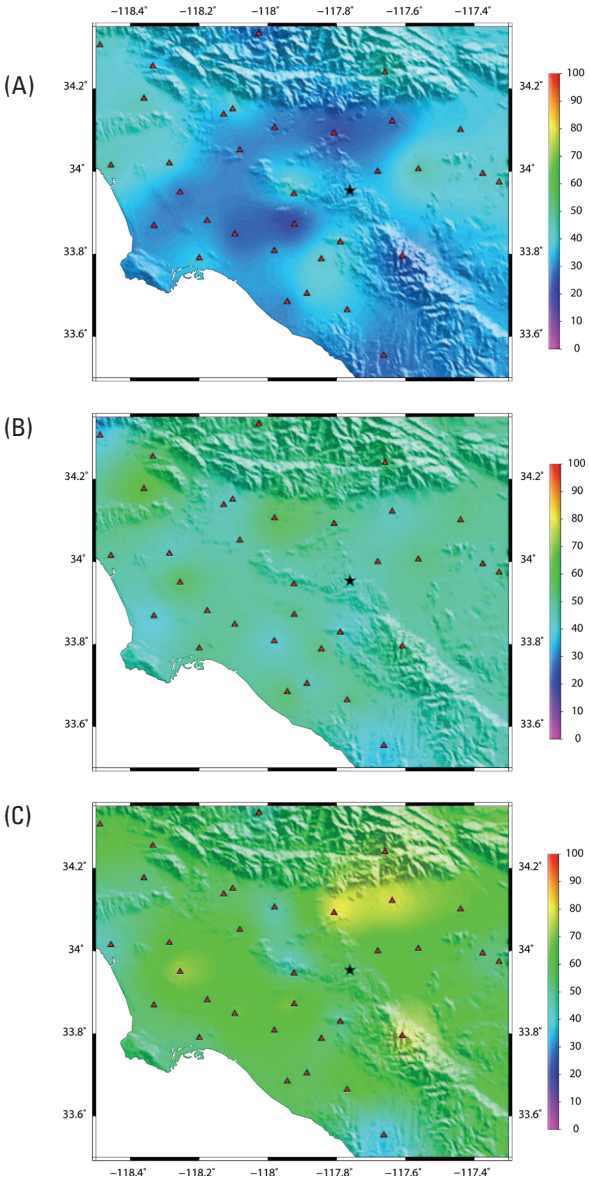

▲ **Figure 5.** GOF maps of IE ratios at A) short periods (0.2–0.5 s), B) moderate periods (0.75–1.5 s) and C) long periods (2.0–5.0 s).

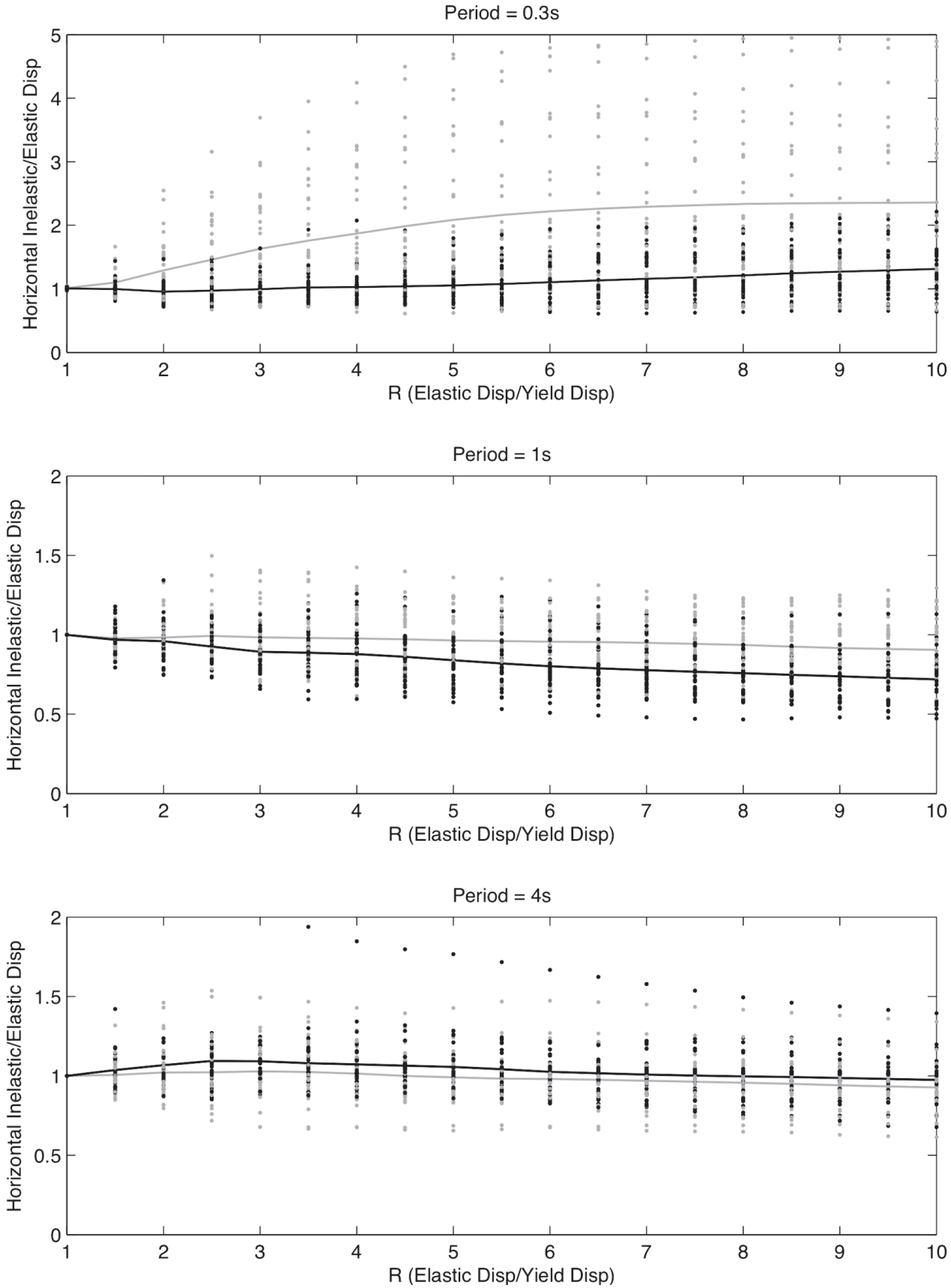

▲ **Figure 6.** IE ratios derived from data (gray symbols) and synthetics (black symbols) at A) 0.3 s, B) 1.0 s, and C) 4.0 s. The dots are mean horizontal IE ratio values calculated for all 33 stations and the solid lines are the corresponding mean values.

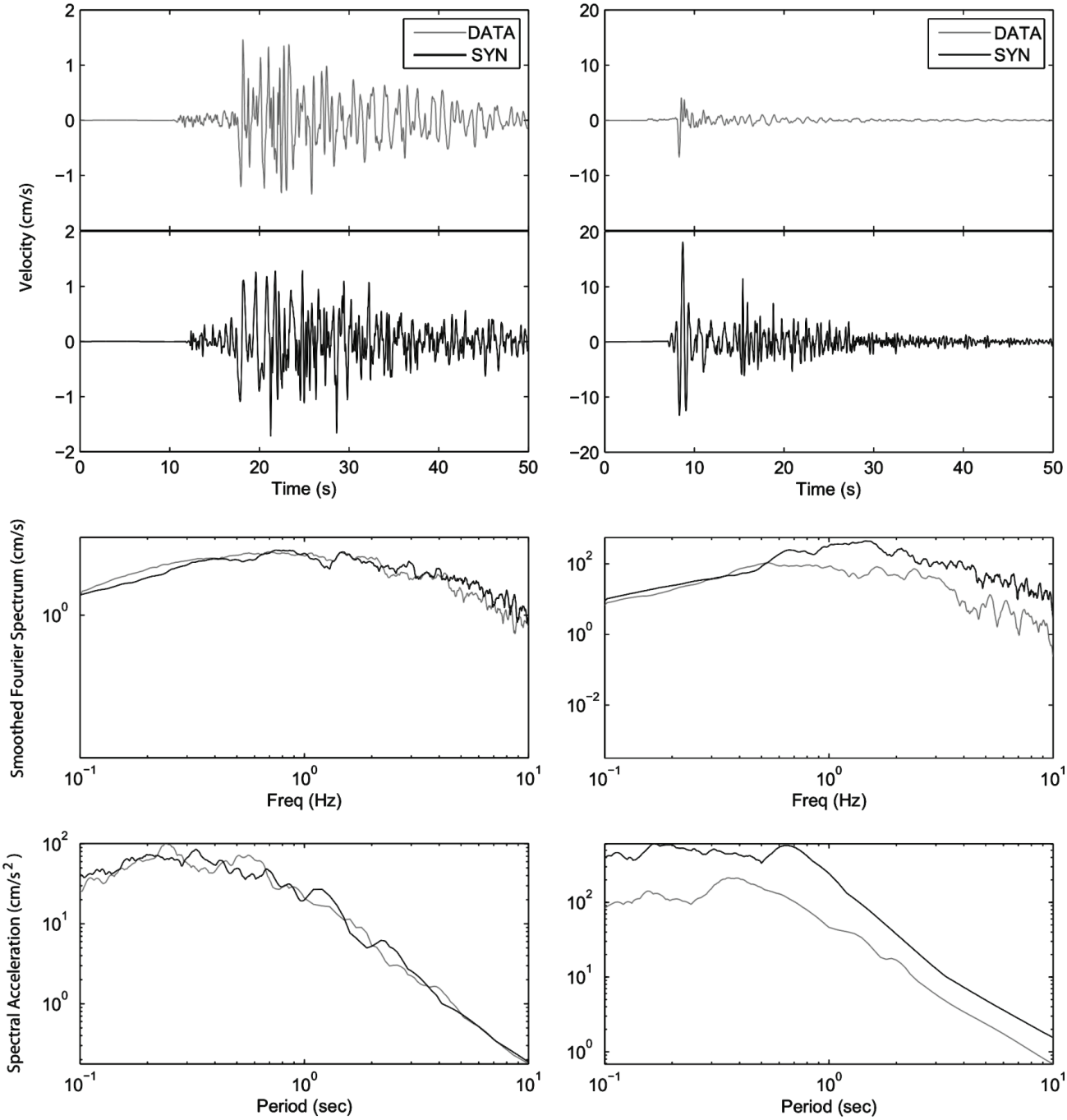

▲ **Figure 7.** Waveform, FS, and RS comparisons for the NS-component synthetic and recorded ground motion for the Chino Hills earthquake at stations HLL (left) and PDU (right). The average broadband, RS, PGV, and FS GOF values are 67, 75, 82, and 51, respectively, at site HLL (left), and 19, 14, 19, and 11, respectively, at site PDU.

SCEC has developed a broadband platform (BBP) to verify and validate different approaches to calculate BBSs, with several different HF generators implemented on the platform. A comparison of the differences between the methods, and between ground-motion intensity measures for the BBSs generated by the method and those from GMPEs, would be greatly facilitated by use of GOF algorithms, such as ours. Finally, the GOF algorithm may help identify errors in the source mechanism determined for recorded earthquakes.

ACKNOWLEDGMENTS

This work is funded by SCEC and through NSF grants including 1) Petascale Cyberfacility for Physics-based Seismic Hazard Analysis Research Project (PetaSHA) (EAR-0623704) and 2) Enabling Earthquake System Science through Petascale Calculations (PetaShake) (OCI-749313). We would like to thank Steven Day for his support and critical reviews. We appreciate the professional input and assistance provided by

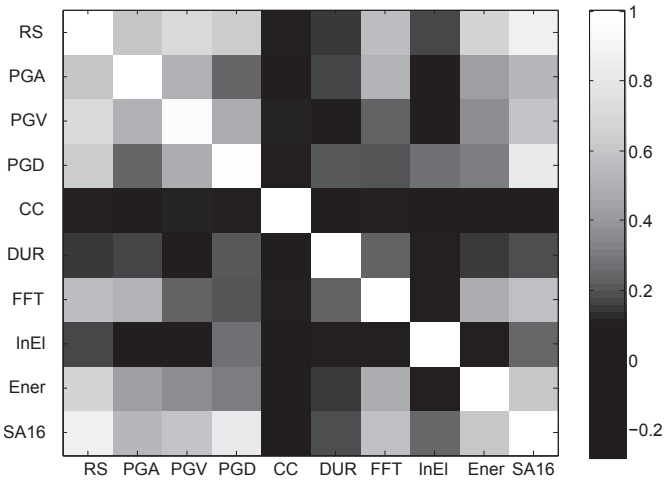

▲ **Figure 8.** Correlation matrix for the ten metrics used by our GOF measure for three-component comparisons at 33 sites (99 GOF values for each metric).

Walter Imperatori, Robert Graves, Jack Baker, and Swami Krishnan. We would also like to thank Yoshifumi Yamamoto for providing NGA relationship code and Nicolas Luco for making his inelastic response spectrum routines available. The data records for the Chino Hills earthquake comparisons were acquired in SAC format from the SCEC data center (http://www.data.scec.org). The Chino Hills source parameters were obtained from the United States Geological Survey Web site. The Chino Hills simulations were generated on the Kraken Cray XT4 supercomputer at University of Tennessee. The GOF algorithm is available from the authors upon request. This is SCEC publication #1430.

REFERENCES

Anderson, J. (2004). Quantitative measure of the goodness-of-fit of synthetic seismograms. In *Proceedings of the 13th World Conference on Earthquake Engineering, Vancouver*, paper 243. Vancouver, B.C., Canada, 1–6 August 2004. Earthquake Engineering Research Institute.

Baker, J. W., and N. Jayaram (2008). Validation of ground motion simulations for engineering applications. In *Proceedings of the SCEC Annual Meeting, Palm Springs* 6–11,September 2008

CalTrans (2008). Damage to Grier St. POC [Br. #53-1158]. Post-earthquake investigation team report, California Department of Transportation, 9/2/2008.

Day, S. M., and C. Bradley (2001). Memory-efficient simulation of anelastic wave propagation. *Bulletin of the Seismological Society of America* **91,** 520–531

Dreger, D., E. Tinti, and A. Cirella (2007). Slip velocity function parameterization for broadband ground motion simulation. *Seismological Research Letters* **78***,* 308 (abstract).

Graves, R., and A. Pitarka (2004). Broadband time history simulation using a hybrid approach. In *Proceedings of the 13th World Conference on Earthquake Engineering, Vancouver*, paper 1098. Vancouver, B.C., Canada, 1–6 August 2004. Earthquake Engineering Research Institute.

Graves, R. W., and P. G. Somerville (2006). Broadband ground motion simulations for scenario earthquakes on the Puente Hills fault. In *Proceedings of the Eighth National Conference on Earthquake Engineering,* San Francisco, California, paper 1052. Oakland, CA: Earthquake Engineering Research Institute.

Hauksson, E., K. Felzer, and D. Given (2008). Preliminary report on the 29 July 2008 *Mw* 5.4 Chino Hills, eastern Los Angeles basin, California, earthquake sequence. *Seismological Research Letters* 7**9**, 855–866.

Jones, L., R. Bernknopf, D. Cox, J. Goltz, K. Hudnut, D. Mileti, S. Perry, D. Ponti, K. Porter, M. Reichle, H. Seligson, K. Shoaf, J. Treiman, and A. Wein (2008). *The ShakeOut Scenario.* USGS Open File Report 2008-1150.

Kristekova, M., J. Kristek, P. Moczo, and S. M. Day (2006). Misfit criteria for quantitative comparison of seismograms. *Bulletin of the Seismological Society of America* **96***,* 1,836–1,850.

Liu, P., R. A. Archuleta, and S. H. Hartzell (2006). Prediction of broadband ground-motion time histories: Hybrid low/high-frequency method with correlated random source parameters. *Bulletin of the Seismological Society of America* **96** (6), 2,118–2,130.

Mai, P. M., and G. C. Beroza (2003). A hybrid method for calculating near-source, broadband seismograms: Application to strong motion prediction. *Physics of the Earth and Planetary Interiors* **137** (1–4), 183–199.

Mai, P. M., W. Imperatori, and K. B. Olsen (forthcoming). Hybrid broadband ground-motion simulations: Combining long-period deterministic synthetics with high-frequency multiple *S*-to-*S* backscattering. *Bulletin of the Seismological Society of America*.

Mena, B., M. Mai, K. B. Olsen, M. D. Purvance, and J. N. Brune (forthcoming). Broadband ground motion simulations for seven large earthquake scenarios on the southern San Andreas fault: Constraints from precariously balanced rocks. *Bulletin of the Seismological Society of America*.

Olsen, K. B., S. M. Day, L. A. Dalguer, J. Mayhew, Y. Cui, J. Zhu, V. M. Cruz-Atienza, D. Roten, P. Maechling, T. H. Jordan, D. Okaya, and A. Chourasia (2009). ShakeOut-D: Ground motion estimates using an ensemble of large earthquakes on the southern San Andreas. *Geophysical Research Letters* **36**, L04303; doi:10.1029/2008GL036832.

Olsen, K. B., S. M. Day, J. B. Minster, Y. Cui, A. Chourasia, D. Okaya, P. Maechling, and T. Jordan (2008). TeraShake2: Simulation of *Mw* 7.7 earthquakes on the southern San Andreas with spontaneous rupture description. *Bulletin of the Seismological Society of America* **98**, 1,162–1,185.

Star, L. M., J. P. Stewart, and R. W. Graves (forthcoming). Comparison of ground motions from hybrid simulations to NGA prediction equations. *Earthquake Spectra*.

Tothong, P., and C. A. Cornell (2006). An empirical ground-motion attenuation relation for inelastic spectral displacement. *Bulletin of the Seismological Society of America* **96**, 2,146–2,164.

San Diego State University
Department of Geological Sciences
5500 Campanile Drive
San Diego, California 92182 U.S.A.
kbolsen@sciences.sdsu.edu
(K. B. O.)